Front. Phys. China (2007) 1: 17−30
DOI 10.1007/s11467-007-0002-y

REVIEW ARTICLE

HUANG Ji-ping

Theory of enhanced second-harmonic generation in some artificial materials

Abstract We review the recent theoretical investigation on enhanced second-harmonic generation (SHG) in soft nonlinear optical materials based on ferrofluids, graded metallic films, and graded metal-dielectric films of anisotropic particles. The SHG of soft ferrofluid-based nonlinear optical materials possess magnetic-field controllabilities, i.e., magnetic-field-controllable anisotropy, red-shift and enhancement, which are caused to appear by the shift of a resonant plasmon frequency due to the formation of the chains of the coated nanoparticles. Both graded metallic films and graded metal-dielectric films of anisotropic particles can serve as a novel optical material for producing a broad structure in both the linear and SHG response and an enhancement in the SHG signal, due to the local field effects.

Keywords second harmonic generation, soft nonlinear optical materials, graded metallic films, graded metal-dielectric films

PACS numbers 42.65.An, 42.79.Ry, 42.70.Nq, 78.20.Bh, 78.66.Vs, 78.67.Pt

1 Introduction

Materials lacking inversion symmetry can exhibit a so-called second order nonlinearity. This can give rise to the phenomenon of second harmonic generation (SHG), i.e., an input (pump) wave can generate another wave with twice the optical frequency (namely, half the wavelength) in the medium. In most cases, the pump wave is delivered in the form of a laser beam, and the second-harmonic wave is generated in the form of a beam propagating in a similar direction. The physical mechanism behind SHG can be understood as follows. Due to the second order nonlinearity, the fundamental (pump) wave generates a nonlinear polarization that oscillates with twice the fundamental frequency. According to Maxwell's equations, this nonlinear polarization radiates an electromagnetic field with this doubled frequency. Due to phase matching issues, the generated second-harmonic field propagates dominantly in the direction of the nonlinear polarization wave. The latter also interacts with the fundamental wave, so that the pump wave can be attenuated (pump depletion) when the second-harmonic intensity develops. In the mean time, energy is transferred from the pump wave to the second-harmonic wave.

With the advancements in nanotechnology, it has become possible to fabricate nanoparticles and composites of various kinds with specific geometries and structures. Either composite effects or gradation effects are expected to open a fascinating field of new phenomena in nonlinear optics. Owing to composite effects, two or more materials can be combined in such a manner that the effective SHG susceptibility of the composite exceeds those of the constituent materials, which is thus called enhanced SHG. Such enhanced SHG can also be caused to appear due to gradation effects. In this article, we shall review our recent theoretical investigation on enhanced second-harmonic generation (SHG) in soft nonlinear optical materials based on ferrofluids, graded metallic films, and graded metal-dielectric films of anisotropic particles, which were theoretically designed in our recent papers [1−7].

HUANG Ji-ping (✉)
Surface Physics Laboratory (National Key Laboratory) and Department of Physics, Fudan University, Shanghai 200433, China
E-mail: jphuang@fudan.edu.cn

Received November 27, 2006

2 Soft nonlinear optical materials based on ferrofluids

Theoretical [8] and experimental [9] reports suggested that spherical particles exhibit a rather unexpected and nontrivial behavior, SHG, due to the broken inversion symmetry at particle surfaces, despite their central symmetry which

seemingly prohibits second-order nonlinear effects. In colloidal suspensions, the SHG response for centrosymmetric particles was experimentally reported [9]. Most recently, the SHG from centrosymmetrical structure has received extensive attention (e.g., see Refs. [10–12]). In view of recent advancements in the fabrication of nanoshells [13, 14] and single domain ferromagnetic nanoparticles [15], we shall theoretically suggest a class of nonlinear optical materials in which single domain ferromagnetic nanoparticles coated by a nonmagnetic nanoshell with an intrinsic SHG susceptibility are suspended in a nonmagnetic host fluid (Fig. 1). For such a material, there is not only an incident light, but also an external magnetic field $\boldsymbol{H}$. The latter yields the formation of chains of coated nanoparticles [16], changing the microstructure of the system and thus yielding the effective SHG with magnetic-field controllabilities. This kind of SHG is expected to receive broad interest in the physics, optics, and engineering communities, because it is difficult or impossible to achieve with conventional, naturally occurring materials or random composites [1, 2, 4, 5, 17, 18].

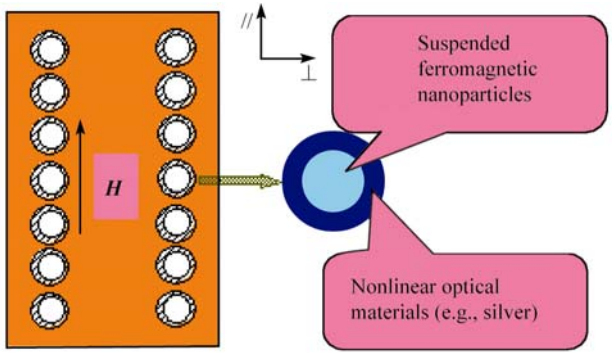

Fig. 1 (*Color online*) Design for a nonlinear optical material, which is subjected to an external magnetic field $\boldsymbol{H}$. // (or ⊥): Longitudinal (or transverse) field cases corresponding to the fact that the E–field of an incident light is parallel (or perpendicular) to the nanoparticle chain. From Ref. [3].

When a collection of objects (e.g., coated nanoparticles or nanoparticle chains) whose size and spacing are much smaller than the wavelength λ of an incident light, the light passing through the structure cannot tell the difference, and hence the inhomogeneous structure can be seen as a homogeneous one [19]. In this regard, to investigate the SHG responses of the proposed material, we are allowed to average over inhomogeneous coated nanoparticles or nanoparticle chains, conceptually replacing the inhomogeneous objects by a homogeneous material (Figs. 2, 3). Let us consider a linear ferromagnetic spherical nanoparticle with dielectric constant ε''_1 and radius r, which is coated by a nonlinear optical nonmagnetic nanoshell (e.g., noble metals like silver or gold) with frequency-dependent dielectric constant $\varepsilon'_1(\omega)$ and intrinsic SHG susceptibility $d_s^{ijk}(-2\omega;\ \omega,\omega)$ with each of the superscripts running over the three Cartesian indices. Here ω denotes the angular frequency of a monochromatic external electric field, and the radius of the whole coated nanoparticle is represented as R in the following. All the coated nanoparticles are suspended in a linear nonmagnetic host fluid of ε_2. In the nanoshell, the local constitutive relation between the displacement field $\boldsymbol{D}_s$ and the electric field $\boldsymbol{E}_s$ in the static case is given by, $D_s^i = \sum_j \varepsilon'_1(\omega)^{ij} E_s^j + \sum_{jk} d_s^{ijk}(-2\omega;\omega,\omega)\, E_s^j E_s^k\,(i = x, y, z)$, where D_s^i and E_s^i are the ith component of $\boldsymbol{D}_s$ and $\boldsymbol{E}_s$, respectively. Here $\varepsilon'_1(\omega)^{ij} = \varepsilon'_1(\omega)\delta_{ij}$ denotes the linear dielectric constant, which is assumed for simplicity to be isotropic. Upon certain symmetry, one can have $d_s^{iii}(-2\omega;\ \omega,\omega) \neq 0 (i = x, y, z)$ as $d_s^{xxx}(-2\omega;\ \omega,\ \omega) = d_s^{yyy}(-2\omega;\omega,\omega) = d_s^{zzz}(-2\omega;\omega,\omega)$. If a monochromatic external field is applied, the nonlinearity in the system will generally generate local potentials and fields at all harmonic frequencies. For a finite-frequency external electric field of the form $E_0 = E_0(\omega)\mathrm{e}^{-\mathrm{i}\omega t} + c.c.$, the equivalent and effective SHG susceptibilities for the coated nanoparticle and the whole suspension, $d_1^{zzz}(-2\omega;\ \omega,\ \omega)$ [Eq. (2)] and $d_e^{zzz}(-2\omega;\omega,\omega)$ [Eq. (4)], can be extracted by considering the volume average of the displacement field at the frequency $2\,\omega$ in the inhomogeneous medium. The electric field $\boldsymbol{E}_s$ in the nanoshell can be calculated [18] using standard electrostatics, by solving the corresponding Maxwell equation $\nabla\times\boldsymbol{E}_s = 0$, which implies that $\boldsymbol{E}_s = -\nabla\phi$, where ϕ is an electric potential. Next, the equivalent linear dielectric constant $\varepsilon_1(\omega)$ for the coated nanoparticle can be given by the Maxwell-Garnett formula [17]:

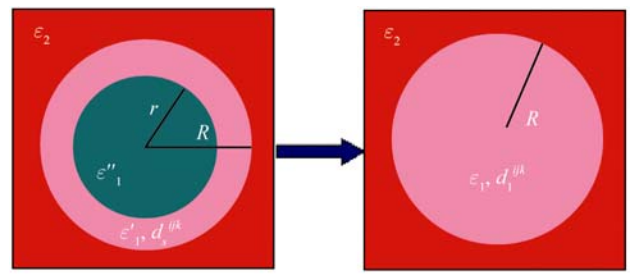

Fig. 2 (*Color online*) Schematic graph showing the equivalence between a coated inhomogeneous nanoparticle (*left*) and a homogeneous nanoparticle (*right*) according to Eqs. (1) and (2). From Ref. [3].

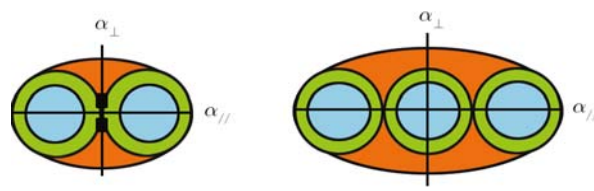

Fig. 3 (*Color online*) Schematic graph showing the quivalence between nanoparticle chains and spheroids with geometrical major-axis (or minor-axis) depolarization factor $\alpha_{//}$ (or $\alpha_{\perp}$) [Eq. (3)]. The major axis is parallel to external magnetic fields. α is also called local magnetic field factors. From Ref. [3].

$$\frac{\varepsilon_1(\omega)-\varepsilon'_1(\omega)}{\varepsilon_1(\omega)+2\varepsilon'_1(\omega)}=(1-f)\frac{\varepsilon''_1-\varepsilon'_1(\omega)}{\varepsilon''_1+2\varepsilon'_1(\omega)} \tag{1}$$

where $f = 1 - r^3 / R^3$ is the volume ratio of the nanoshell to the whole coated nanoparticle. The Maxwell-Garnett formula is a well-known asymmetrical effective medium theory, and may thus be valid for a low concentration of nanoparticles in composites [20]. While treating a single coated nanoparticle with full range $0 \leqslant f \leqslant 1$, the Maxwell-Garnett formula [Eq. (1)] holds for the calculation of $\varepsilon_1(\omega)$ indeed, due to the natural existence of asymmetry in the coated nanoparticle. The solution of $\boldsymbol{E}_s$ in Ref. [18] can be used to derive the equivalent SHG susceptibility for the coated nanoparticle, $d_1^{iii}(-2\omega;\ \omega,\ \omega)$,

$$d_1^{iii}(-2\omega;\omega,\omega)=fd_s^{iii}(-2\omega;\omega,\omega)\sum_{j=x}^{z}\left\langle\frac{E_{s,j}(2\omega)}{E_{0,i}(2\omega)}\left(\frac{E_{s,j}(\omega)}{E_{0,i}(\omega)}\right)^2\right\rangle_s \tag{2}$$

where $\langle\cdots\rangle_s$ denotes a volume average over the nanoshell. To show the feature of the proposed material, we assume the optical responses [namely, $\varepsilon_1(\omega)$ and $d_1^{iii}(-2\omega;\omega,\omega)$] of an equivalent spheroid or a chain (see Fig. 3) to be the same as those of each coated nanoparticle inside the spheroid or chain. For convenience, the suspension is further assumed to be the one that contains identical equivalent spheroids with geometrical depolarization factor $\alpha_{//}$ (or $\alpha_\perp$) along major (or minor) axis (Fig. 3). In the following, α is also called *local magnetic field factors*, because, from the physical point of view, the spheroids (or chains) are just formed due to the application of external magnetic fields. In this connection, the summation term in Eq. (2) admits

$$\{\Pi(2\omega)\Pi^2(\omega)+(4/5)(rR)^{-3}[\Pi(2\omega)p_s^2(\omega)+2\Pi(\omega)p_s(2\omega)p_s(\omega)]+(8/35)(r^3+R^3)/(r^6R^6)p_s(2\omega)p_s^2(\omega)\}/[E_{0,i}(2\omega)E_{0,i}^2(\omega)]$$

where $\Pi(\omega)=T_s(\omega)E_{0,i}(\omega)$ and $p_s(\omega)=b_s(\omega)r^3\,T_s(\omega)E_{0,i}(\omega)$ with $b_s(\omega)=(\varepsilon''_1-\varepsilon'_1(\omega))/(\varepsilon''+2\varepsilon'_1(\omega))$ and $T_s(\omega)=\{\Theta(\omega)+2b_s(\omega)[\Theta(\omega)-1](1-f)\}^{-1}$. Here $\Theta(\omega)=[\varepsilon'_1(\omega)+2\varepsilon_2]/(3\varepsilon_2)$.

In the following analysis, we assume that the spheroidal particle possess the same linear response as the coated particle. But, for the nonlinear response, to include the shape effect, let us introduce a local magnetic field factor α that denotes $\alpha_{//}$ and $\alpha_\perp$ for longitudinal and transverse field cases, respectively (Figs. 1 and 3). There is a sum rule for $\alpha_{//}$ and $\alpha_\perp$, $\alpha_{//}+2\alpha_\perp=1$ [21]. The parameter α measures the degree of structural anisotropy due to the formation of nanoparticle chains, which is induced to appear by the external magnetic field $\boldsymbol{H}$. More precisely, the degree of the magnetic-field-induced anisotropy is measuredby how much α deviates from 1/3, $1/3<\alpha_\perp<1$ and $0<\alpha_{//}<1/3$. As H increases, $\alpha_\perp$ and $\alpha_{//}$ should tend to 1 and 0, respectively, which is indicative of the formation of longer nanoparticle chains (or equivalent spheroids). Therefore, α should be a function of external magnetic fields H. Specifically, for $H = 0$ there is $\alpha_{//}=\alpha_\perp=1/3$, which corresponds to an isotropic system in which all the coated nanoparticles are randomly distributed in the suspension. After the introduction of α, while we assume the spheroid possess the same nonlinear response as the coated particle, for more accurate estimation of the nonlinear response of the spheroid, let us replace $\Theta(\omega)=[\varepsilon'_1(\omega)+2\varepsilon_2]/(3\varepsilon_2)$ with $\Theta(\omega)=[\varepsilon_2+\alpha(\varepsilon'_1(\omega)-\varepsilon_2)]/\varepsilon_2$. That is, the shape effect of spheroids has been included. Apparently, the substitution of $\alpha=1/3$ into Eq. (2) yields the same expression as the Eq. (15) in Ref. [18] in which a random composite of particles with nonlinear nonmetallic shells was investigated. Alternatively, according to the calculation of major-axis depolarization factor L of prolate spheroids [21], $L=1/(1-\rho^2)+\rho/(\rho^2-1)^{3/2}\ln(\rho+\sqrt{\rho^2-1})$, where $\rho(>1)$ is the ratio between the major and minor axes of the elliptic cross section, α can be given in terms of the number n of nanoparticles in an equivalent spheroid (or a chain):

$$\alpha_{//}=\frac{1}{1-n^2}+\frac{n}{(n^2-1)^{3/2}}\ln(n+\sqrt{n^2-1}) \tag{3}$$

Throughout this section (Section 2), while both the nanoshell and host fluid are nonmagnetic, the core is ferromagnetic. The existence of ferromagnetism in the core makes the chain formation possible, as long as an external magnetic field H is applied [16]. We have added the magnetic contribution to the expressions for optical responses through the local magnetic field factor α. So far the exact relation between α and H is not known because it relates to complicated suspension hydrodynamics and kinetics at nonequilibrium. Nevertheless, the results obtained from Fig. 4 are valid for equilibrium systems in which neither hydrodynamics nor kinetics can affect the SHG. Without loss of any generality, to capture the features and their physics of the proposed materials, in Fig. 4 we use α to represent the strength of the external magnetic field H.

Now we see the suspension as the one in which the equivalent spheroids with $\varepsilon_1(\omega)$ [Eq. (1)] and $d_1^{iii}(2\omega;\ \omega,\omega)$ [Eq. (2)] are embedded in the host fluid. Owing to the z-directed external magnetic field, all the spheroids should also be directed along the z axis, but with the locations being randomly distributed. According to the general expression for the effective SHG susceptibility [18], we take one step forward to express the effective SHG susceptibility $d_e^{iii}(-2\omega;\omega,\omega)$ for the whole suspension in the dilute limit,

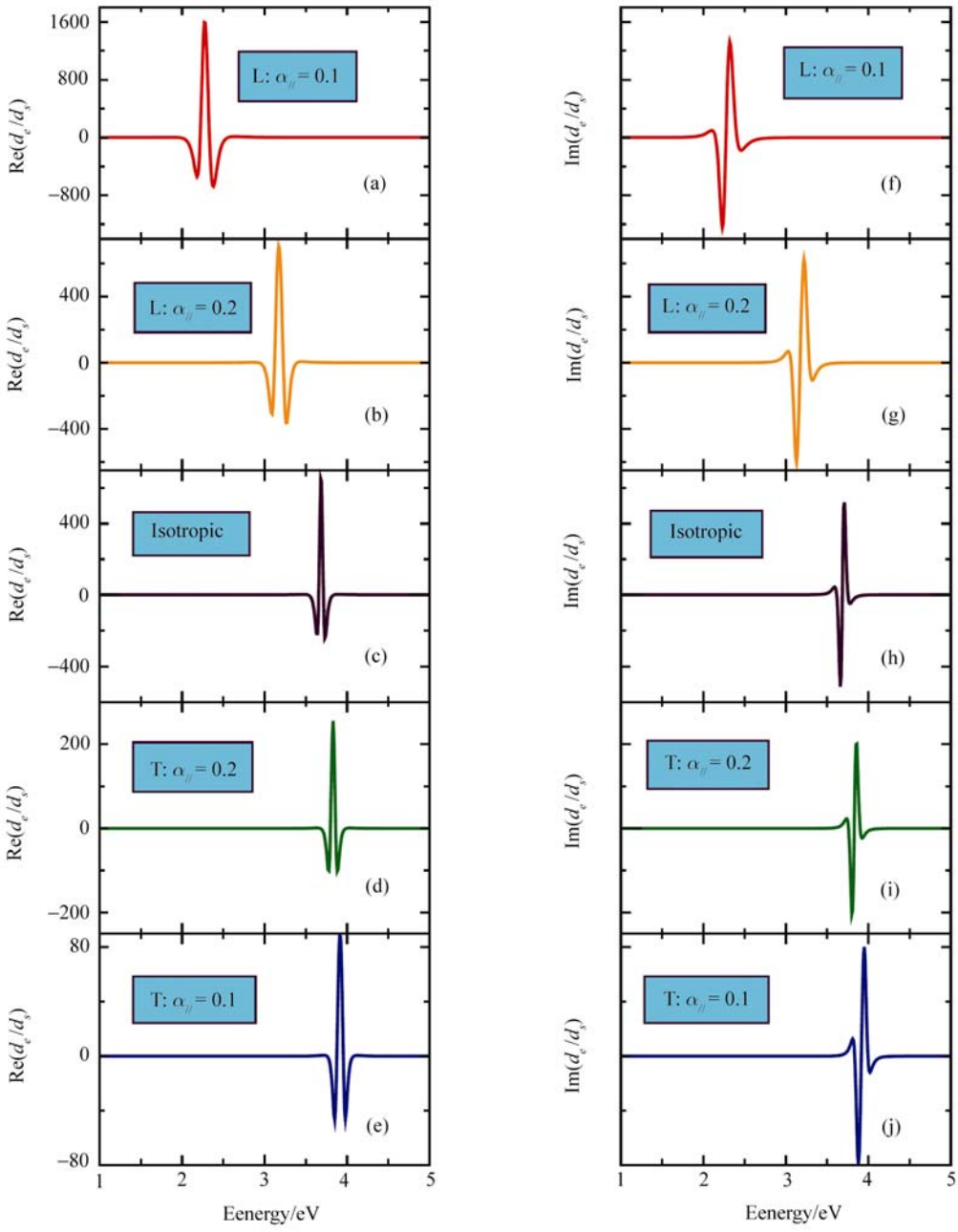

Fig. 4 (*Color online*) The **(a)** − **(e)** real and **(f)** − **(j)** imaginary parts of the effective SHG susceptibility $d_e^{iii}(-2\omega;\omega,\omega) \equiv d_e$ normalized by the intrinsic SHG susceptibility in the nonlinear nanoshell $d_s^{iii}(-2\omega;\omega,\omega) \equiv d_s$, for different external magnetic fields represented by local magnetic field factors $\alpha_{//}$, versus the energy of an incident light. Here "L" and "T" denote the longitudinal and transverse field cases, respectively. According to Eq. (3), the number n of nanoparticles in the chains is $n \approx 3$ for $\alpha_{//} = 0.1$ and $n \approx 2$ for $\alpha_{//} = 0.2$. Note in **(d)**, **(e)**, **(i)** and **(j)** the corresponding $\alpha_{\perp}$ in use can be calculated according to the relation $\alpha_{//} + 2\alpha_{\perp} = 1$. From Ref. [3].

$$d_e^{iii}(-2\omega;\omega,\omega) = p d_1^{iii}(-2\omega;\omega,\omega)\Gamma(2\omega)\Gamma^2(\omega) \qquad (4)$$

where p is the volume fraction of the coated nanoparticles. In Eq. (4), $\Gamma(\omega)$ is a local electric field enhancement factor, and it is obtained by deriving the factor in a spheroid of depolarization factor α with principle axes along external electric fields, $\Gamma(\omega) = \varepsilon_2 / [\varepsilon_2 + \alpha(\varepsilon_1(\omega) - \varepsilon_2)]$.

Since metal surfaces were used to obtain enhanced SHG

responses [22], for our numerical simulations we take a Drude dielectric function (that is valid for noble metals within the frequency range of interest) for $\varepsilon'_1(\omega), \varepsilon'_1(\omega) = \varepsilon(\infty) - (\varepsilon(0) - \varepsilon(\infty))\omega_p^2 / [\omega(\omega + i\gamma)]$, where ω_p is the bulk plasmon frequency (which is proportional to the surface plasmon frequency ω_{sp}, e.g., $\omega_p = \sqrt{3}\omega_{sp}$ for a sphere [23]), $\varepsilon(\infty)$ the high-frequency limit dielectric constant, $\varepsilon(0)$ the static dielectric constant, and γ the collision frequency. Specifically, for silver, $\varepsilon(\infty) = 5.45, \varepsilon(0) = 6.18$, and $\omega_p = 1.72\times10^{16}$ rad/s [24]. In addition, we take $\gamma = 0.01\omega_p$ (a typical value for metals), r = 5 nm (a typical value for single domain ferromagnetic nanoparticles [16]), the thickness of nanoshells 1.9 nm (or R = 6.9 nm), $\varepsilon''_1 = -25 + 4i$ (e.g., for cobalt), frequency-independent dielectric constant $\varepsilon_2 = 1.77$ (high-frequency limit dielectric constant of water), and p = 0.18. Based on the values of r, R and p, we obtain the volume fractions, p_c and p_s, of the ferromagnetic and nonlinear optical components in the whole suspension, p_c = 0.07 and p_s = 0.11, according to the relations $R / r = (1 + p_s / p_c)^{1/3}$ and $p = p_c + p_s$. We shall investigate the light energy 1 ~ 5 eV, which corresponds to the wavelength $\lambda = 248 \sim 1242$ nm, or the frequency range $\omega = 1.52\times10^{15} \sim 7.59\times10^{15}$ rad/s.

We show the effective SHG susceptibility $d_e^{iii}(-2\omega;\omega,\omega)$ of the whole suspensions in Fig. 4. For longitudinal field cases [Fig. 4 (a), (b), (f), and (g)], as $\alpha_{//}$ decreases (i.e., external applied magnetic field H increases, and longer nanoparticle chains are formed accordingly), the resonant peak in the SHG response is not only red-shifted (namely, located at a lower frequency), but also further enhanced, when compared to the isotropic case at zero external magnetic field H = 0 [Fig. 4 (c) and (h)]. However, inverse behavior appears for transverse field cases [Fig. 4 (d), (e), (i), and (j)]. In detail, for transverse field cases, as the external magnetic field increases, the resonant peak in the SHG signal is both reduced and blue-shifted (i.e., located at higher frequency), and hence becomes less attractive.

It turns out generally difficult to give a full account of all the numerical results in simple physical terms. When the magnetic field is applied, the coated nanoparticles will form chains, thus changing the microstructure of the system accordingly. For longitudinal field cases, the nonlinear component will become more abundant along the chains than perpendicular to the chains for transverse field. When there is an incident light, the nonlinear component in the system will generally generate local potentials and fields at all harmonic frequencies. The formation of nanoparticle chains due to the application of external magnetic fields changes the surrounding circumstance of each coated nanoparticle naturally, which in turn affects the local electric field in the nanoshells and hence shifts the resonant plasmon frequency at which the resonant peak appears (Fig. 4). Therefore, in the presence of an external magnetic field, the SHG response becomes anisotropic (i.e., its strength in the longitudinal field differs from that in the transverse field), and the degree of anisotropy can further be adjusted by tuning the external magnetic field. That is, the SHG response of the system can be affected accordingly.

Optical absorption arises from the surface plasmon resonance, which is obtained from the imaginary part of the effective dielectric constant. For single metallic particles in the dilute limit, it is well known that there is a large absorption when the resonant condition $\varepsilon'_1 + 2\varepsilon_2 = 0$ is fulfilled. When there is a volume fraction p of structured particles and an anisotropy α of the suspension, the effective dielectric constant might be obtained from the Maxwell-Garnett approximation, thus yielding a modified resonant condition $(1 - 3p\alpha)\varepsilon_1 + (2 + 3p\alpha)\varepsilon_2 = 0$. So, the resonant frequency becomes smaller (larger) than the isotropic limit (α = 1/3) when α becomes smaller (larger) than 1/3. In other words, there is a red (blue) shift for the longitudinal (transversal) field cases. In this section (Section 2), there is no an additional spectral feature in the SHG spectrum at the subharmonic of the surface-plasmon resonance frequency, similar to that displayed in Fig. 1 of Ref. [18]. In Ref. [18], the authors numerically calculated a system in which a linear core (Drude metal) coated with a nonlinear dielectric shell. However, we discuss a different system in which linear core coated with a nonlinear shell (Drude metal). Such difference might be used to explain the lack of signal at the subharmonic of this resonance.

Since the permanent magnetic moment of magnetite nanoparticles m is approximately $2.4\times10^4\,\mu_B$ (where μ_B denotes the Bohr magneton) [16], we can estimate the threshold magnetic field H_c = 14.3 kA/m (or threshold magnetic induction B_c = 0.018 T) above which the corresponding magnetic energy can overcome the thermal energy 1/40 eV so as to obtain appreciable anisotropy. It is worth noting that $B_c \gg B_{c0} (\sim 10^{-4}\,\mathrm{T})$ where B_{c0} means the earth's magnetic induction. Thus, the earth's magnetic field cannot induce anisotropic structure inside the system of interest. Besides the magnetic energy, we should also consider the interaction energy. For two touching magnetite nanoparticles, the interaction between them is proportional to $m^2 / (2R)^3$, assuming the two coated particles to be in a head-to-tail alignment. Since the magnetic moment m goes as $(2r)^3$, the interaction energy could vary as $(2r^2/R)^3$. In order to break up the touching nanoparticles, the thermal energy should be larger than the interaction energy. So, threshold field H_c = 14.3 kA/m serves as an upper estimate, whereas for cobalt nanoparticles the threshold field H_c should be lower due to larger permanent magnetic moments inside them.

In looking for experimental evidence, we note that Du and Luo have reported nonlinear optical effects in suspen-

sions of ferromagnetic nanoparticles (with mean diameter 9 nm) in kerosene [25]. They observed that the nonlinear optical effect is enhanced by applying a moderate magnetic field. However, this mechanism was unclear at that time. Based on the present section (Section 2), it seems that this enhanced nonlinear optical effect results from the magnetic field-induced anisotropic structure.

Our results obtained from Fig. 4 are valid for equilibrium systems in which neither hydrodynamics nor kinetics can affect the SHG (For a non-equilibrium system, complex hydrodynamics and kinetics should be taken into account). In this section (Section 2), we have not included the effect of distributions of the number of nanoparticles in chains. Nevertheless, based on the same physics/mechanism, it is not difficult to understand that the SHG signal can become broad (not as sharp as in Fig. 4) once the distribution is taken into account. Without external fields, such materials show a giant nonlinearity enhancement, due to the local field effect. In external magnetic fields, the materials have anisotropic nonlinear optical properties. By adjusting the external fields, the obtained optical responses is red-shifted (blue-shifted) in longitudinal (transverse) field cases. In case of an external magnetic field, the nonlinear optical properties can further be enhanced in the corresponding suspension. The approach (i.e., using external magnetic fields to get magnetic-field-induced structural anisotropy and hence obtain the desired SHG) described in this section (Section 2) should also be expected to stimulate future research on developing or designing optical materials that stay in a rapidly changing field. If one needs to include the effect of quantum confinement, the quantitative, rather than qualitative, results might be improved somehow. So, we have presented a simplified picture to study the seemingly complicated problem, with a focus on discovering new features and their physics of the proposed material.

In this section (Section 2), we have assumed the dielectric function of nanoparticles to be size-independent, in order to focus on the main aim that the SHG response can be magnetic-field-controllable. If we use different r (inner radius) and R (outer radius), quantitative results can be changed naturally, while the qualitative results we have achieved will remain unchanged.

Here we should remark that the Drude function of use is invalid in the range 3.5–5 eV for silver due to the onset of interband transitions. For this range, the Drude function could be improved by including the effect of interband electron transitions [26], and fortunately our results (i.e., overall magnitude, anisotropy, and frequency shifting of the second-harmonic response) remain qualitatively unchanged. In other words, the results obtained in this section (Section 2) are not only valid for ideal Drude metals, but also qualitatively reasonable for real metals like silver.

We have also assumed that the dipolar contribution dominates the system. This assumption might be reasonable because the number of particles in the chains used for the present numerical calculations is very small, namely 2 or 3 only. For more particles in the chains, the multipolar contribution will become more important.

We have investigated the effective SHG susceptibility resulting from an intrinsic nonlinear characteristic only. Since the concentration of the magnetic component used in the calculations is very small, namely, 7 %, the role of the net magnetization might be expected to be less important in comparison with the contribution from the intrinsic nonlinear characteristic. On the other hand, if the role of the net magnetization becomes significant (e.g., in a system with higher concentration of the magnetic component), the SHG signal obtained from the proposed materials is expected to become somehow more interesting.

In summary, the proposed materials possess SHG with magnetic-field controlabilities, which is expected to be valuable for optical applications like optical limiters, optical switches, etc.

3 Graded metallic films

There have been recent interest and practical need for nonlinear optical materials that process large nonlinear susceptibility or optimal figure of merit. A large enhancement in nonlinear responses has been found for a sub-wavelength multiplayer (i.e., thin film) of titanium dioxide and conjugated polymer [27]. For nonlinear effects other than the Kerr effect, Hui *et al*. [28] derived general expressions for the effective susceptibility for the second-harmonic generation (SHG) in a binary composite of random dielectrics. They have also studied the thickness dependence of effective SHG susceptibility in films of random dielectrics and in composites with coated small particles [18, 29]. Graded materials with various functionalities appear in nature and in fabricated materials. Graded thin films have many applications as the gradation profile provides an additional control on the physical properties. Graded thin films often possess different optical properties [30], when compared to bulk materials. It is known that graded materials have quite different physical properties from the homogeneous materials [31]. Also, it has been observed that the compositionally graded barium strontium titanate thin films have better electric properties than a single-layer barium strontium titanate film with the same compositions [32]. How to achieve enhanced SHG is up to now a challenging agenda [33, 34]. In this section (Section 3), we shall investigate SHG in a graded metallic film (Fig. 5) with an intrinsic SHG response and a graded linear response in the metallic dielectric function.

Fig. 5 Sketch showing a graded metallic film with a gradient along z axis perpendicular to the film. The electric field $\boldsymbol{E}$ is parallel to the gradient along z axis.

Let us consider a graded metallic film with thickness L, with the gradation profile in the direction perpendicular to the film. If we only include quadratic nonlinearities, the local constitutive relation between the displacement field $\boldsymbol{D}(z)$ and the electric field $\boldsymbol{E}(z)$ in the static case would be $D_i(z) = \sum_j \varepsilon_{ij}(z)E_j(z) + \sum_{jk} \chi_{ijk}(z)E_j(z)E_k(z)$ [18, 29] with $i = x$, y, z, where $D_i(z)$ and $E_i(z)$ are the ith component of $\boldsymbol{D}(z)$ and $\boldsymbol{E}(z)$, respectively, and χ_{ijk} is the SHG susceptibility. Here, $\varepsilon_{ij}(z)$ denotes the linear dielectric function, which we assume for simplicity to be isotropic $\varepsilon_{ij}(z) = \varepsilon(z)\delta_{ij}$. Both $\varepsilon(z)$ and $\chi_{ijk}(z)$ are functions of z and describe the gradation profiles. In general, when a monochromatic external field is applied, the nonlinearity will generate local potentials and fields at all harmonic frequency. For a finite frequency external electric field of the form $E_0 = E_0(\omega)\, e^{-i\omega t} + c.c.$, the effective SHG susceptibility $\bar{\chi}_{2\omega}$ can be extracted by considering the volume average of the displacement field at the frequency 2ω in the inhomogeneous medium [18, 28, 29]. Next, we adopt a graded dielectric profile that follows the Drude form:

$$\varepsilon(z,\omega) = 1 - \frac{\omega_p^2(z)}{\omega[\omega + i\gamma(z)]} \tag{5}$$

where $0 \leqslant z \leqslant L$. The general form in Eq. (5) allows for the possibility of a gradation profile in the plasma frequency [e.g., Eq. (8)] and the relaxation rate [e.g., Eq. (9)]. For a z-dependent profile, we can make use of the equivalent capacitance for capacitors in series to evaluate the effective perpendicular linear response for a given frequency, $1/\bar{\varepsilon}(\omega) = (1/L)\int_0^L dz[1/\varepsilon(z,\omega)]$. Using the continuity of the electrical displacement field, the local electric fields $E(z, \omega)$ satisfies

$$\varepsilon(z,\omega)E(z,\omega) = \bar{\varepsilon}(\omega)E_0(\omega) \tag{6}$$

where $E_0(\omega)$ is the applied field along the z axis. A z-dependent profile for the plasma frequency and the relaxation time can be achieved experimentally. One possible way may be to impose a temperature profile, as it has been observed that surface enhanced Raman scattering is sensitive to temperature [35]. Thus, one may tune the surface plasmon frequency by imposing an appropriate temperature gradient [23]. A temperature gradient may also be used in materials with a small band gap or with a profile on dopant concentrations. In this case, one may impose a charge carrier concentration profile to a certain extent. This effect, when coupled with materials with a significant intrinsic nonlinear susceptibility, will give us a way to control the effective nonlinear response. For less conducting materials, one may replace the Drude form of dielectric constants by a Lorentz oscillator form. It may also be possible to fabricate dirty metal films in which the degree of disorder varies in the z-direction and hence leads to a relaxation-rate gradation profile.

The calculation of the effective nonlinear optical response then proceeds by applying the expressions derived in Refs. [2, 3]. Next, the effective SHG susceptibility $\bar{\chi}_{2\omega}$ is given by $\bar{\chi}_{2\omega} = \left\langle \chi_{2\omega}(z)E_{\text{lin}}(z,2\omega)E_{\text{lin}}(z,\omega)^2 \right\rangle \Big/ [E_0(2\omega)E_0(\omega)^2]$, where E_{lin} is the linear local electric field in the graded film with the same gradation profile but with a vanishing nonlinear response at the frequency concerned. Using Eq. (6) for the linear local fields, the effective SHG susceptibility can be rewritten as an integral over the film as:

$$\bar{\chi}_{2\omega} = \frac{1}{L}\int_0^L dz\, \chi_{2\omega}(z) \cdot \frac{\bar{\varepsilon}(2\omega)}{\varepsilon(z,2\omega)} \cdot \left[\frac{\bar{\varepsilon}(\omega)}{\varepsilon(z,\omega)}\right]^2 \tag{7}$$

To illustrate the SHG in graded films, we consider as a model system that the intrinsic SHG susceptibility $\chi_{2\omega}(z) = \chi_1$ to be a real and positive frequency-independent constant and does not have a gradation profile. In doing so, we are allowed to focus on the enhancement of the SHG response when compared to χ_1. To show the effects of gradation, here we take as a model plasma-frequency gradation profile

$$\omega_p(z) = \omega_p(0)(1 - C_\omega \cdot z) \tag{8}$$

and a model relaxation-rate gradation profile [36]:

$$\gamma(z) = \gamma(\infty) + C_{\gamma/z} \tag{9}$$

where C_ω and C_γ are constant parameters tuning the profile, which is assumed to be linear in z. Here $\gamma(\infty)$ denotes the bulk damping coefficient, i.e., for $z \to \infty$ Set thickness L = 1 so that we could focus on the film with a fixed thickness. Regarding the thickness dependence, we refer the reader to the work by Hui *et al*. [29].

Figure 6 shows the real and imaginary parts of the effective linear dielectric constant [Fig. 6 (a) and (b)], and the real and imaginary parts of the effective SHG susceptibility [Fig. 6 (c) and (d)] as a function of frequency $\omega/\omega_p(0)$. Also shown is the modulus of $\bar{\chi}_{2\omega}/\chi_1$, see Fig. 6 (e). The dielectric function gradation profile is given in Eqs. (5), (8) and (9) with $C_\gamma = 0$, i.e., only a graded plasmon frequency is included. Throughout the calculations, the real part of the (linear) dielectric constant is negative naturally. In this case, a broad resonant plasmon band is observed. Note that for $C_\omega \to 0$, $\omega_p(z)/\omega_p(0) \to 1$. As C_ω increases, $\omega_p(z)$ takes on values within a broader range across the film, and leads to a broad plasmon band. Increasing C_ω also causes the plasmon peak to shift to lower frequencies. The reason is that, analogous to capacitors in series, the effective dielectric constant of the film is dominated by the layer with the smallest dielectric constant. For the SHG response, the frequency dependence is quite complicated. As C_ω increases, it is noted that structures in the SHG response also shifts to the lower frequencies and the range of values of the SHG

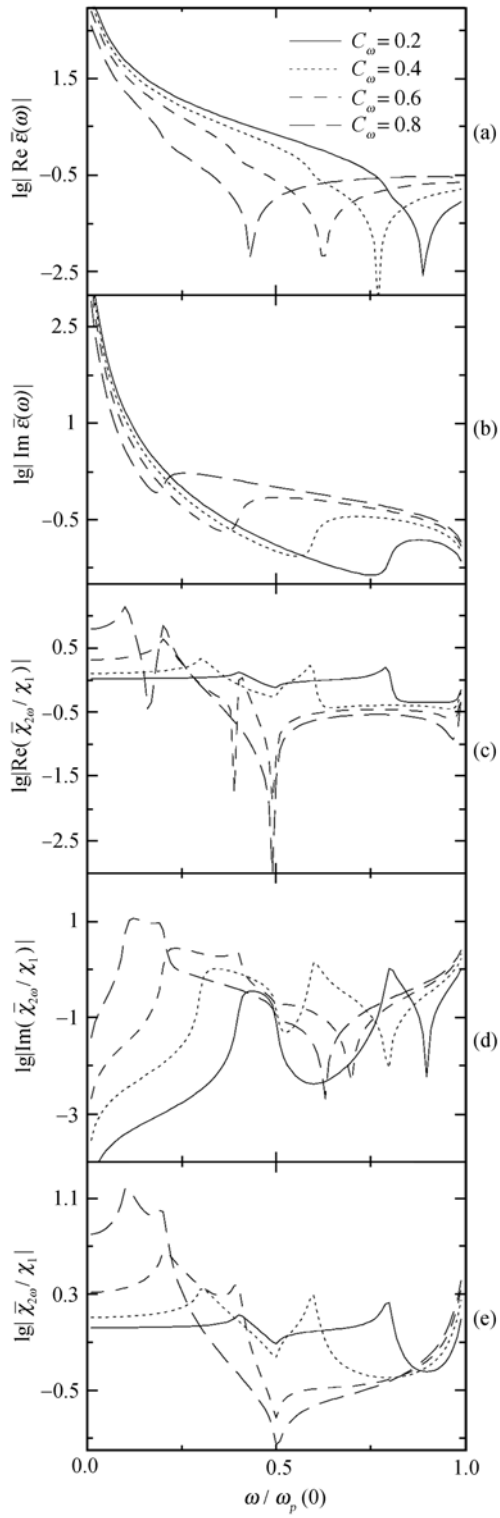

Fig. 6 **(a)** Re $\bar{\varepsilon}(\omega)$, **(b)** Im $\bar{\varepsilon}(\omega)$ (linear optical absorption), **(c)** Re ($\bar{\chi}_{2\omega}/\chi_1$), **(d)** Im($\bar{\chi}_{2\omega}/\chi_1$), and **(e)** Modulus of $\bar{\chi}_{2\omega}/\chi_1$ versus the normalized incident angular frequency ω/ω_p (0) for the dielectric function gradation profile [Eq. (5)] with various plasma-frequency gradation profile [Eq. (8)] and relaxation-rate gradation profile [Eq. (9)]. Here $|\cdots|$ denotes the absolute value or modulus of $\cdots$. Parameters: $\gamma(\infty) = 0.02\omega_p(0)$ and $C_\gamma = 0.0$. From Ref. [6].

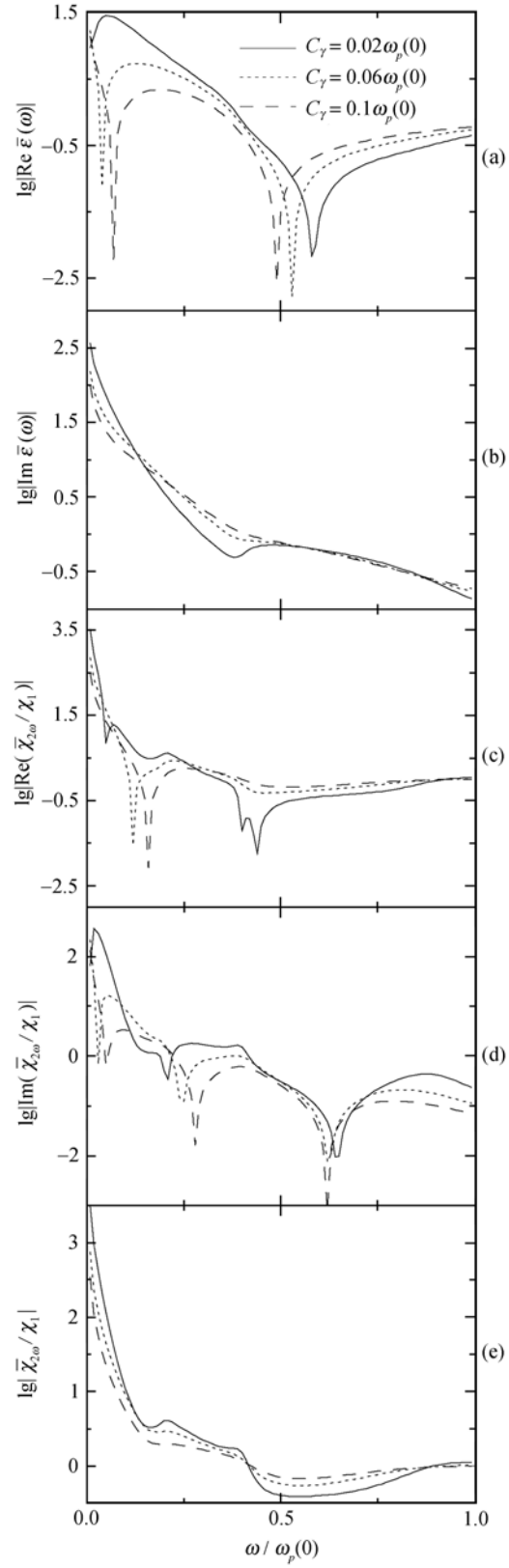

Fig. 7 Same as Fig. 6. Parameters: $\gamma(\infty) = 0.02\omega_p(0)$ and $C_\omega = 0.6$. From Ref. [6].

susceptibility increases as well. Figure 7 displays the results of model calculations in which a gradation profile of the relaxation rate of the form in Eq. (9) is also included. The effects are similar to those in Fig. 6. The SHG response is found to be enhanced more strongly in the presence of both a relaxation-rate gradation and a plasma-frequency gradation (see Fig. 6) than for plasmon-frequency gradation alone, especially at low frequencies. As C_γ increases, the structures in the linear and SHG response both show a shift to lower frequencies. In Figs. 6 and 7, the quantities, which can be both positive and negative, are plotted in logarithm of modulus. When the quantities pass through zero, the logarithm will be very large, thus yielding spikes. In addition, we have used the normalized numbers in order to describe a general origin of the SHG in metal films rather than a specified metal film.

The point for achieving the present results is that one needs a sufficiently large gradient rather than a crucially particular form of the dielectric function or gradation profiles. Thus, it is expected that an enhancement in SHG responses will also be found in compositionally graded metal-dielectric composite films in which the fraction of metal component varies perpendicular to the film. In the present section (Section 3), due to the symmetry of the film, we only have enhancement for the polarization perpendicular to the film (i.e., parallel to the direction of the gradient). In this polarization, the tangential component of the electric field E vanishes identically. Thus, the continuity of the normal component of D [see Eq. (6)] gives rise to the enhanced SHG. However, for the polarization parallel to the film, i.e., the tangential component does not vanish. In this polarization, it is the continuity of the tangential component of E that leads to no enhancement at all [27].

4 Graded metal-dielectric films of anisotropic particles

Nonlinear optical materials with an appreciable nonlinear susceptibility or optimal figure of merit (FOM) [37–39] are of importance in industrial applications such as nonlinear optical switching devices in photonics and real-time coherent optical signal processors. In general, many applications of nonlinear optics that have been demonstrated under controlled laboratory conditions could become practical for technological uses if such materials were available. Much work has been done on how to achieve a substantial nonlinear optical response or/and optimal FOM in bulk metal-dielectric composites, by invoking the surface-plasmon resonance [40–42] and by incorporating structural effects [1, 4, 27, 43]. For nonlinear phenomena in Kerr composites, the nonlinear alternating current responses have been investigated [44–48]. For nonlinear effects other than the Kerr effect, Hui *et al*. [28] derived general expressions for the effective susceptibility for the second-harmonic generation (SHG) in a binary composite of random dielectrics. Recently, these authors have also studied the thickness dependence of the effective SHG susceptibility in films of random dielectrics [29] and the enhancement in the SHG in dilute composites of coated small particles [18].

Graded materials with various functionalities appear in nature and in fabricated materials. These materials have many applications as the gradation profile provides an additional means of controlling the physical properties. In other words, graded materials could have quite different physical properties from homogeneous materials [1, 6, 31, 49–53]. To achieve desired optical responses, the technique of gradation is expected to be useful for a variety of optical materials, e.g., metal-dielectric composites and negative- refractive-index metamaterials [19–54]. In particular, graded thin films often possess different optical properties, when compared with a film processing the same properties at different locations along the growth direction. For example, a large enhancement in nonlinear optical responses was found in a composite of alternating, sub-wavelength-thick layers of titanium dioxide and conjugated polymer [27], which can be regarded as a graded material. It has also been observed that compositionally graded barium strontium titanate thin films have better electric properties than a single-layer barium strontium titanate film with the same composition [32].

Crucial elements for controlling the linear and nonlinear optical properties of metal-dielectric composites include the micro-structure of the composite, particle shape, and the properties of the constituents. For anisotropically shaped metallic nanoparticles, the resonant plasmon bands split for orientations along the major and minor axes. In the case of a large size aspect ratio, the plasmon bands may shift downward in frequency into the infrared, thus enabling the possible use of metal nanostructures in telecommunication applications. When compared with spherically shaped particles, anisotropically shaped metallic particles show reduced plasmon relaxation times [55] as well as enhanced nonlinear responses [56], and may thus be used as building blocks in a variety of optical devices. Experimentally, techniques have been developed to fabricate rod-shaped metallic nanoparticles by using lithographic means [57] or anisotropic growth. Recently, it has been demonstrated that ion irradiation in the energy range of mega-electron-volt (MeV) can also be used to modify the shape of nanoparticles [58]. This ion-beam-induced anisotropic deformation effect is known to occur not only in a wide range of amorphous materials [59], but also in crystalline materials including metals [60]. With this advancement in experimental techniques, samples of spheroidal metallic particles randomly dispersed in a dielectric host can readily be prepared.

To achieve an enhanced and controllable SHG in functional optical materials is still a challenging task (see Refs. [6, 34] and references therein). In this section (Section 4), we investigate the effects of gradation and/or particle shape on the SHG response in graded metal-dielectric films. In these films, the volume fraction of the anisotropically shaped metallic particles varies in the direction perpendicular to the film, i.e., along the growth direction of the film.

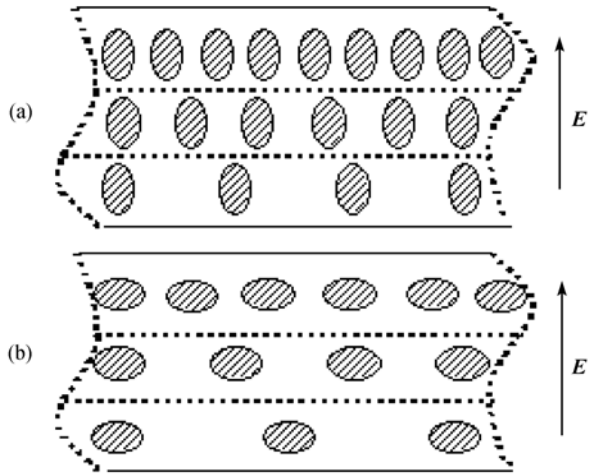

Fig. 8 Schematic graph showing the geometry of a graded metal-dielectric composite film with a variation of volume fraction of **(a)** prolate and **(b)** oblate spheroidal metallic particles along the z axis perpendicular to the film. The electric field E is parallel to the gradient along the z axis. From Ref. [7].

We consider a graded metal-dielectric composite film of thickness L, with the gradation profile in the direction (z-direction) perpendicular to the film (Fig. 8). If one considers quadratic nonlinearities only, the local constitutive relation between the displacement field $\boldsymbol{D}(z)$ and the electric field $\boldsymbol{E}(z)$ in the static case is given by [18, 29]:

$$D_i(z) = \sum_j \varepsilon_{ij}(z) E_j(z) + \sum_{jk} \chi_{ijk}(z) E_j(z) E_k(z), \quad i = x, y, z \tag{10}$$

where $D_i(z)$ and $E_i(z)$ are the ith component of $\boldsymbol{D}(z)$ and $\boldsymbol{E}(z)$, respectively, and χ_{ijk} the SHG susceptibility. Here $\varepsilon_{ij}(z) = \varepsilon(z)\delta_{ij}$ denotes the linear dielectric constant, which is assumed for simplicity to be isotropic. Both $\varepsilon(z)$ and $\chi_{ijk}(z)$ are functions of z, as a result of the gradation profile in the z-direction.

If a monochromatic external field is applied, the nonlinearity in the system will generally generate local potentials and fields at all harmonic frequencies. For a finite frequency external electric field of the form

$$E_0 = E_0(\omega) \mathrm{e}^{-\mathrm{i}\omega t} + c.c. \tag{11}$$

the effective SHG susceptibility $\bar{\chi}_{2\omega}$ can be extracted by considering the volume average of the displacement field at the frequency 2ω in the inhomogeneous medium [6, 18, 28, 29].

Let $p(z)$ be the volume fraction of the metallic component in the graded film. To calculate $\varepsilon(z,\omega)$, we invoke the well-known Maxwell-Garnett approximation [61]:

$$\frac{\varepsilon(z,\omega) - \varepsilon_2}{L_z \varepsilon(z,\varepsilon) + (1 - L_z)\varepsilon_2} = p(z) \frac{\varepsilon_1(\omega) - \varepsilon_2}{L_z \varepsilon_1(\omega) + (1 - L_z)\varepsilon_2} \tag{12}$$

where $\varepsilon_1(\omega)$ and ε_2 are the linear dielectric constants of the metallic and dielectric components, respectively. Here, L_z is the depolarization factor describing the anisotropy of the metallic particles along the z-axis, with $0 < L_z < 1/3$ (or $1/3 < L_z < 1$) denoting prolate (or oblate) spheroids and $L_z = 1/3$ for spherical particles [49]. It is worth noting that prolate spheroidal particles can more easily be fabricated than oblate spheroidal particles in experiments using the method of ion irradiation (see, e.g., Ref. [60]). For completeness, we discuss both prolate and oblate spheroidal particles (Fig. 9). Implicit in Eq. (12) is the assumption that the major axes of the metallic particles are aligned perpendicular to the film. Experimentally, prolate spheroidal metallic particles can be made highly oriented along the direction of irradiated ions [60].

The dielectric function $\varepsilon_1(\omega)$ of the metallic component is taken to be the Drude form:

$$\varepsilon_1(\omega) = 1 - \frac{\omega_p^2}{\omega(\omega + \mathrm{i}\gamma)} \tag{13}$$

where ω_p denotes the plasma frequency and γ the relaxation rate. For a z-dependent volume fraction profile $p(z)$, we can make use of the equivalent capacitance for capacitors in series to evaluate the effective perpendicular linear dielectric response $\bar{\varepsilon}(\omega)$ at a given frequency, i.e.,

$$\frac{1}{\bar{\varepsilon}(\omega)} = \frac{1}{L} \int_0^L \frac{\mathrm{d}z}{\varepsilon(z,\omega)} \tag{14}$$

The treatment of the effective linear response is analogous to the effective medium approximation for the thermal properties of graded films [52].

The calculation of the effective nonlinear optical response proceeds by applying the expressions derived in Ref. [28]. The effective SHG susceptibility $\bar{\chi}_{2\omega}(z)$ for the slice of the system at position z is given by [18, 29]:

$$\bar{\chi}_{2\omega}(z) = p(z) \chi_{2\omega} \alpha(z, 2\omega) [\alpha(z,\omega)]^2 \tag{15}$$

where $\alpha(z, \omega)$ denotes the local-field factor in a *linear* inhomogeneous system [28] which, for consistency with Eq. (12) in getting $\varepsilon(z,\omega)$, should also be determined by using the Maxwell-Garnett approach. The result is

$$\alpha(z,\omega) = \frac{\varepsilon_2}{\varepsilon_2[1 - L_z(1 - p(z))] + \varepsilon_1(\omega) L_z (1 - p(z))} \tag{16}$$

In Eq. (15), $\chi_{2\omega}$ is the intrinsic SHG susceptibility of the metallic component. For simplicity, we assumed that the dielectric host is linear. The effective SHG susceptibility $\bar{\chi}_{2\omega}$ of the whole film can then be evaluated by a one-dimensional integral over the film thickness to give

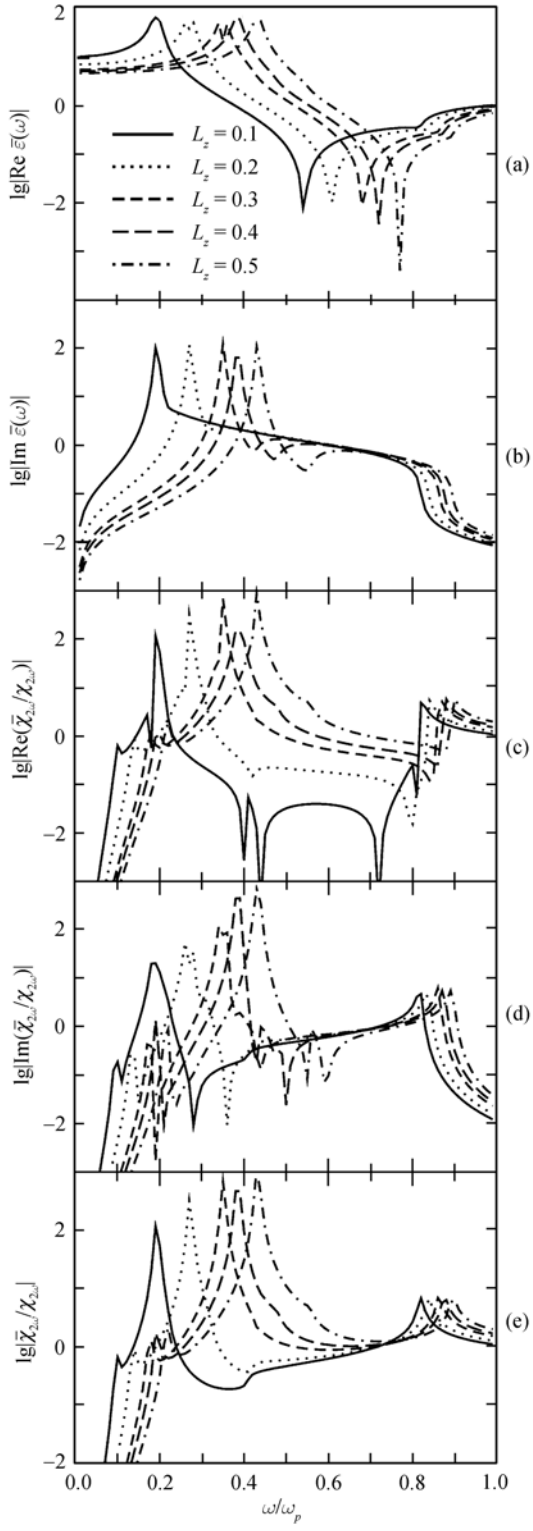

Fig. 9 **(a)** Re $\bar{\varepsilon}(\omega)$, **(b)** Im $\bar{\varepsilon}(\omega)$ (linear optical absorption), **(c)** Re($\bar{\chi}_{2\omega}/\chi_{2\omega}$), **(d)** Im($\bar{\chi}_{2\omega}/\chi_{2\omega}$), and **(e)** Modulus of $\bar{\chi}_{2\omega}/\chi_{2\omega}$, versus the normalized incident angular frequency ω/ω_p for layer metal profile $p(z) = az^m$, for different L_z. Here $|\cdots|$ denotes the absolute value or modulus of $\cdots$. Parameters: $a = 0.8$, $m = 1$, $\gamma/\omega_p = 0.01$, and $\varepsilon_2 = (3/2)^2$. From Ref. [7].

$$\bar{\chi}_{2\omega} = \frac{1}{L}\int_0^L \mathrm{d}z\,\bar{\chi}_{2\omega}(z)\cdot\frac{E(z,2\omega)}{E_0}\cdot\left[\frac{E(z,\omega)}{E_0}\right]^2 \tag{17}$$

where $E(z,\omega)$ denotes the volume average of the electric field within a layer at position z.

By virtue of the continuity of electric displacement, there is a relation

$$\varepsilon(z,\omega)E(z,\omega) = \bar{\varepsilon}(\omega)E_0 \tag{18}$$

Thus, we obtain

$$\bar{\chi}_{2\omega} = \frac{1}{L}\int_0^L \mathrm{d}z\,\bar{\chi}_{2\omega}(z)\cdot\frac{\bar{\varepsilon}(2\omega)}{\varepsilon(z,2\omega)}\cdot\left[\frac{\bar{\varepsilon}(\omega)}{\varepsilon(z,\omega)}\right]^2 \tag{19}$$

Equation (19), coupled with Eqs. (12) and (14), gives a compact expression for the effective SHG susceptibility in graded films.

For illustration, we take a model profile of metallic volume fraction of the form:

$$p(z) = az^m \tag{20}$$

where a and m are constants tuning the profile. Without loss of generality, the thickness L is set to unity, i.e., thickness is measured in units of L. Given values of m and a corresponding to a certain volume fraction p of metallic component in the film,

$$p = \frac{1}{L}\int_0^L p(z)\mathrm{d}z \tag{21}$$

For a given profile $p(z)$, if we randomly disperse the *same* amount of anisotropic metallic component in a film of thickness L, the effective SHG susceptibility χ_0 for the *random* film would be [18, 29]

$$\chi_0 = p\chi_{2\omega}\alpha(2\omega)[\alpha(\omega)]^2 \tag{22}$$

where the local-field factor $\alpha(\omega)$ is given by an expression similar to Eq. (16) as:

$$\alpha(\omega) = \frac{\varepsilon_2}{\varepsilon_2[1-L_z(1-p)]+\varepsilon_1(\omega)L_z(1-p)} \tag{23}$$

By comparing the effective SHG susceptibility $\bar{\chi}_{2\omega}$ with χ_0 (see Fig. 10), we can see whether a graded film gives an enhanced SHG response, when compared to a non-graded film of random composite with the *same* volume fraction of metallic component.

We have carried out model numerical calculations to investigate the effects on the local field factors in Eq. (15) due to the gradation profile, the metallic particle shape, and the difference in the linear dielectric response between the two constituents. Figure 9 shows the effects of different degrees of anisotropy as specified by different values of the depolarization factor L_z. Figure 9 gives the real and imaginary parts of the effective linear dielectric constant $\bar{\varepsilon}(\omega)$ [Fig. 9 (a) and (b)], and the real and imaginary parts of the effective SHG susceptibility $\bar{\chi}_{2\omega}$ [Fig. 9 (c) and (d)] as a function of frequency ω/ω_p. Also shown is the modulus

of $\bar{\chi}_{2\omega}/\chi_{2\omega}$ [see Fig. 9 (e)]. For Fig. 9 (and Fig. 10), we take the parameters a = 0.8 and m = 1, which correspond to the total volume fraction p = 0.4 according to Eq. (21). As L_z decreases, i.e., as the shape of the particles changes from oblate spheroid, to sphere, and then to prolate spheroid, the plasmon band becomes broader, and also shifts to lower frequencies, see Fig. 9 (b). In Fig. 9 (c) − (e), $\bar{\chi}_{2\omega}$ is normalized by the intrinsic SHG susceptibility of the metallic component $\chi_{2\omega}$, which is assumed to be a real and positive frequency-independent constant. In Fig. 9 (c) − (e), there exists a frequency range in which a significantly enhanced SHG susceptibility results, when compared with $\chi_{2\omega}$. As L_z decreases, the frequency range becomes narrower and red-shifted to lower frequencies [see Fig. 9 (c) − (e)].

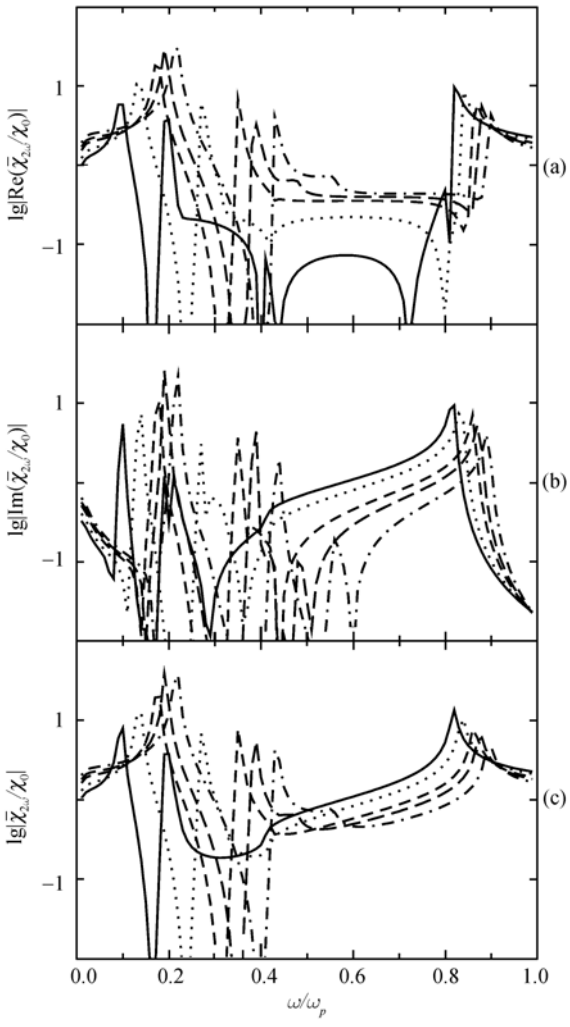

Fig. 10 Same as Fig. 9 **(c)** − **(e)**, respectively, but **(a)** Re($\bar{\chi}_{2\omega}/\chi_0$), **(b)** Im ($\bar{\chi}_{2\omega}/\chi_0$), and **(c)** Modulus of $\bar{\chi}_{2\omega}/\chi_0$. From Ref. [7].

It is also illustrative to compare the results in the presence of a gradation profile with that of a random composite film consisting of the same amount of metallic (nonlinear) component. In Fig. 10, we show the results for $\bar{\chi}_{2\omega}/\chi_0$, where χ_0 is given by Eq. (22). The results indicate that a gradation profile may not always enhance the SHG response. Generally speaking, one has to carefully make sure of the dielectric contrast, together with composition and gradation profiles, to achieve SHG enhancement in certain ranges of frequencies.

To further investigate the effects of a gradation profile, we consider a fixed volume fraction p of the nonlinear component. For a profile of the form $p(z) = az^m$, Eq. (21) implies that the parameters a and m are related by $p = a/(m+1)$. For a given value of p, we may adjust m (and a) to study the effects of different gradation profiles corresponding to the same value of p. Note that m = 0 refers to a non-graded random film. Figure 11 shows the results at the fixed frequency of ω/ω_p = 0.2 for different profiles characterized by the parameter m, for four different values of volume fraction p = 0.1, 0.2, 0.3, and 0.4. The linear responses can be enhanced to a different extent with a gradation profile [see Fig. 11 (a) and (b)]. The imaginary part of the linear dielectric response [Fig. 11 (b)] shows a broad structure with frequency with a broad peak at frequencies at which the real part shows a sharp drop [Fig. 11 (a)], except for the system with the lowest concentration of nonlinear component. Figure 11 (c) − (e) shows that the SHG responses are highly sensitive to the gradation profile. For the same concentration, one may tune the effective response by tuning the concentration profile. Note that for a range of m above m = 0 [see Fig. 11 (e)], there is an increase in the SHG response with m for systems with $p > 0.1$, showing that a suitable gradation profile, which amounts to suitably placing a certain fraction of the nonlinear component in the system, may provide an optimal SHG response for a given fraction of the nonlinear component. Our results show that for small total volume fraction p ($p < 0.1$), a uniform profile or a profile that increases rapidly at small z is beneficial, while for moderate p ($p > 0.1$), there exists an optimal profile for SHG response. Note that for a given total volume fraction p, a gradation profile leads to non-trivial response in that the volume fraction p (z) may be below the percolation threshold for the same values of z and above the threshold for other values of z. Results of our model calculations show that a gradation profile is an additional means for tuning the local field effects.

In the present section (Section 4), we have investigated compositionally graded metal-dielectric composite films in which the fraction of the metallic component varies perpendicular to the film. Enhancement in the response was found for the polarization perpendicular to the film (i.e., parallel to the direction of the gradient), as a result of the continuity of the normal component of the displacement field. For the polarization parallel to the film, the physics is then governed by the continuity of the tangential component of the electric field [27]. It is also instructive to extend the present consideration to metal-dielectric composites in which the inclusion particles are graded particles, i.e., having a radial dielectric gradient. In this case, traditional theories [62] have to be

modified. To this end, a differential effective dipole approximation or a first-principles approach can be used to study composites of graded particles [50]. Including nonlinear response into the consideration, it is expected that an enhanced SHG signal will result in a composite consisting of graded particles.

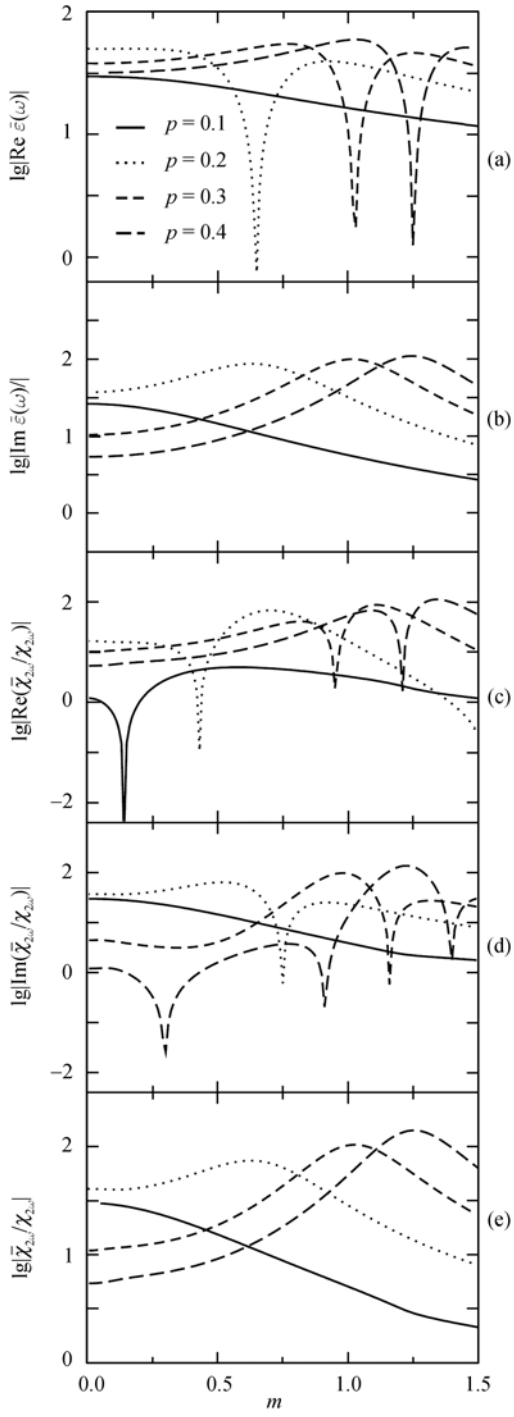

Fig. 11 Same as Fig. 9, but versus m (dimensionless) for different total volume fraction p. Parameters: $L_z = 0.1$, $\omega/\omega_p = 0.2$, $\gamma/\omega_p = 0.01$, and $\varepsilon_2 = (3/2)^2$. From Ref. [7].

5 Summary

We have investigated the physical processes of the composite effect and/or gradation effect on the enhanced SHG responses of soft nonlinear optical materials based on ferrofluids, graded metallic films, and graded metal-dielectric films of anisotropic particles. The SHG of soft ferrofluid-based nonlinear optical materials possess magnetic-field controllabilities, i.e., magnetic-field-controllable anisotropy, red-shift and enhancement, which are caused to appear by the shift of a resonant plasmon frequency due to the formation of the chains of the coated nanoparticles. Both graded metallic films and graded metal-dielectric films of anisotropic particles can serve as a novel optical material for producing a broad structure in both the linear and SHG response and an enhancement in the SHG signal, due to the local field effects. We believe that it is of great value to apply soft matter techniques, so that one could easily fabricate new nonlinear optical materials, and then purposely obtain different optical phenomena like anisotropic and enhanced nonlinear responses.

Acknowledgements This work was financially supported by the Shanghai Education Committee and the Shanghai Education Development Foundation ("Shu Guang" project), by the Pujiang Talent Project (No. 06PJ14006) of the Shanghai Science and Technology Committee, and by the National Natural Science Foundation of China under Grant No. 10604014. We thank Professor K. W. Yu, Professor P. M. Hui and Ms. C. Z. Fan for fruitful discussions and collaboration.

References

1. Huang J. P. and Yu K. W., Physics Reports, 2006, 431: 87
2. Huang J. P. and Yu K. W., New Nonlinear Optical Materials: Theoretical Research, Nova Science Publishers, Inc., New York, 2007, to be published
3. Fan C. Z. and Huang J. P., Appl. Phys. Lett., 2006, 89: 141906
4. Huang J. P. and Yu K. W., Appl. Phys. Lett., 2005, 86: 041905
5. Huang J. P. and Yu K. W., Appl. Phys. Lett., 2004, 85: 94.
6. Huang J. P. and Yu K. W., Opt. Lett., 2005, 30: 275
7. Huang J. P., Hui P. M., and Yu K. W., Phys. Lett. A, 2005, 342: 484
8. Dadap J. I., Shan J., Eisenthal K. B., and Heinz T. F., Phys. Rev. Lett., 1999, 83: 4045
9. Yang N., Angerer W. E., and Yodh A. G., Phys. Rev. Lett., 2001, 87: 103902
10. Xu P., et al., Phys. Rev. Lett., 2004, 93: 133904
11. Bernal R. and Maytorena J. A., Phys. Rev. B, 2004, 70: 125420
12. Gao L. and K. W. Yu, Phys. Rev. B, 2005, 72: 075111
13. Mitzi D. B., Kosbar L. L., Murray C. E., Copel M., and Afzali A., Nature (London), 2004, 428: 299
14. Nehl C. L., et al., Nano Lett., 2004, 4: 2355
15. Puntes V. F., Gorostiza P., Aruguete D. M., Bastus N. G., and Alivisatos A. P., Nat. Mater., 2004, 3: 263
16. Odenbach S., Magnetoviscous Effects in Ferrofluids, Springer, Berlin, 2002

17. Boyd R. W., Nonlinear Optics, Academic Press, New York, 1992
18. Hui P. M., Xu C., and Stroud D., Phys. Rev. B, 2004, 69: 014203
19. Smith D. R., Pendry J. B., and M. Wiltshire C. K., Science, 2004, 305: 788
20. Bergman D. J. and Stroud D., Solid State Physics: Applied in Research and Applications, volume 46, page 147, Academic Press, New York, 1992
21. Landau L. D., Lifshitz E. M., and Pitaevskii L. P., Electrodynamics of Continuous Media, Pergamon Press, New York, 2 Ed., 1984
22. Stockman M. I., Bergman D. J., Anceau C., Brasselet S., and Zyss J., Phys. Rev. Lett., 2004, 92: 057402
23. Chiang H. -P., Leung P. T., and Tse W. S., J. Phys. Chem. B, 2000, 104: 2348
24. Kik P. G., Maier S. A., and Atwater H. A., Phys. Rev. B, 2004, 69: 045418
25. Du T. and Luo W., Appl. Phys. Lett., 1998, 72: 272
26. Shalaev V. M., Phys. Rep., 1996, 272: 61
27. Fischer G. L., et al., Phys. Rev. Lett., 1995, 74: 1871
28. Hui P. M. and Stroud D., J. Appl. Phys., 1997, 82: 4740
29. Hui P. M., Xu C., and Stroud D., Phys. Rev. B, 2004, 69: 014202
30. Grull H., Schreyer A., Berk N. F., Majkrzak C. F., and Han C. C., Europhys. Lett., 2000, 50: 107
31. Milton G. W., The Theory of Composites, Cambridge University Press, Cambridge, England, 2002
32. Lu S. G., et al., Appl. Phys. Lett., 2003, 82: 2877
33. Pezzetta D., et al., J. Opt. Soc. Am. B, 2002, 19: 2102
34. Purvinis G., et al., Opt. Lett., 2004, 29: 1108
35. Pettinger B., Bao X., Wilcock I. C., Muhler M., and Ertl G., Phys. Rev. Lett., 1994, 72: 1561
36. Neeves A. E. and Birnboim M. H., J. Opt. Soc. Am. B, 1989, 6: 787
37. Sekikawa T., Kosuge A., Kanai T., and Watanabe S., Nature (London), 2004, 432: 605
38. Rodenberger D. C., Heflin J. R., and Garito A. F., Nature (London), 1992, 359: 309
39. Butcher P. N. and Cotter D., The Elements of Nonlinear Optics, Cambridge University Press, New York, 1990
40. Yuen K. P. and Yu K. W., J. Opt. Soc. Am. B, 1997, 14: 1387
41. Sahimi M., Heterogeneous Materials I, Springer-Verlag, New York, 2003
42. Sahimi M., Heterogeneous Materials II, Springer-Verlag, New York, 2003
43. Sipe J. E. and Boyd R. W., Phys. Rev. A, 1992, 46: 1614
44. Gu G. Q., Hui P. M., and Yu K. W., Physica B, 2000, 279: 62
45. Wei E. B., Song J. B., and Gu G. Q., J. Appl. Phys., 2004, 95: 1377
46. Wei E. B., Yang Z. D., and Gu G. Q., J. Phys. D: Appl. Phys., 2004, 37: 107
47. Huang J. P., J. Phys. Chem. B, 2005, 109: 4824
48. Huang J. P., Frontal Polymer Research, Nova science publishers, Inc., New York, 2006：131−170
49. Jones T. B., Electromechanics of Particles, Cambridge University Press, Cambridge, England,1995
50. Dong L., Gu G. Q., and Yu K. W., Phys. Rev. B, 2003, 67: 224205
51. Gu G. Q. and Yu K. W., J. Appl. Phys., 2003, 94: 3376
52. Hui P., Zhang X., and Stroud D., J. Mater. Sci., 1999, 34: 5497
53. Wei E., Poon Y., and Shin F., Phys. Lett. A, 2005, 336: 264
54. Sang Z. F. and Li Z. Y., Phys. Lett. A, 2005, 334: 422
55. SÄonnichsen C. et al., Phys. Rev. Lett., 2002, 88: 077402
56. Yuen K. P., Law M. F., Yu K. W., and Sheng P., Phys. Rev. E, 1997, 56: R1322
57. Zande B. M. I. V. D., Pages L., Hikmet R. A. M., and Blaaderen A. V., J. Phys. Chem. B, 1999, 103: 5761
58. Snoeks E., et al., Adv. Mater., 2000, 12: 1511
59. Benyagoub A., et al., Nucl. Instr. Methods Phys. Res. B, 1992, 64: 684
60. Roorda S., et al., Adv. Mater., 2004, 16: 235
61. Bohren C. F. and Huffman D. R., Absorption and Scattering of Light by Small Particles, John Wiley & Sons, New York, 1983
62. Jackson J. D., Classical Electrodynamics, Wiley, New York, 1975